



Levels and sources of hydrocarbons in the Patos Lagoon estuary and Cassino Beach mud bank (South Atlantic, Brazil): evidence of transference between environments

Patricia Andrade Neves · Patricia G. Costa ·
Luana C. Portz · Marina R. Garcia ·
Gilberto Fillmann

Received: 18 July 2022 / Accepted: 2 March 2023 / Published online: 18 March 2023
© The Author(s), under exclusive licence to Springer Nature Switzerland AG 2023

Abstract This study assessed the concentrations and sources of natural and anthropogenic aliphatic (AHs) and polycyclic aromatic hydrocarbons (PAHs) in superficial sediments collected along the Patos Lagoon estuary and in sediment cores obtained from the Cassino Beach mud bank. Levels and distribution of *n*-alkanes indicate terrestrial sources, overlapping with a low amount of petrogenic hydrocarbons (heavy oils). Unresolved complex mixture (UCM) was observed in all samples. On the other hand, the distribution of PAHs in the sediments showed a

predominance of pyrolytic over petrogenic sources. In general, hydrocarbons (HCs) contamination in the Patos Lagoon estuary and its adjacent coastal area can be considered low, except for sites near urban or industrial effluents, where moderate to high levels of contamination were found. Concentrations of hydrocarbons were homogeneous throughout the sediment cores, suggesting that mixing processes may have occurred along the layers or that HCs inputs to the mud banks were uniform during the studied deposition period. In addition, the levels and profile of HCs in the coastal sediments were similar to those observed in the estuary. Moreover, the frequent remobilization of sediments from the mud bank towards Cassino beach does not seem to pose any threats to

Supplementary Information The online version contains supplementary material available at <https://doi.org/10.1007/s10661-023-11074-3>.

P. A. Neves · P. G. Costa · L. C. Portz · M. R. Garcia (✉) ·
G. Fillmann (✉)
Instituto de Oceanografia, Universidade Federal
de Rio Grande (FURG), Av. Itália km 8, s/n,
RS 96203-900 Rio Grande, Brazil
e-mail: marinareback@gmail.com

G. Fillmann
e-mail: gfillmann@furg.br; gfillmann@gmail.com

P. A. Neves · P. G. Costa · G. Fillmann
Programa de Pós-Graduação em Oceanologia,
Universidade Federal do Rio Grande, Av. Itália km 8, s/n,
RS 96203-900 Rio Grande, Brazil

P. A. Neves
Universidade de São Paulo, Instituto Oceanográfico,
Laboratório de Química Orgânica Marinha, Praça do
Oceanográfico 191, 05508-120 São Paulo, SP, Brazil

L. C. Portz
Universidad Autonoma de Madrid, Ciudad Universitaria
de Cantoblanco, 28049 Madrid, Spain

M. R. Garcia
Programa de Pós-Graduação em Sistemas Costeiros e
Oceânicos, Universidade Federal do Paraná, Caixa Postal
61, PR 83255-976 Pontal do Paraná, Brazil

M. R. Garcia
Centro de Estudos do Mar da Universidade Federal
do Paraná, Caixa Postal 61, 83255-976 Pontal do Paraná,
PR, Brazil

the local biota or beach users since the levels of contamination were relatively low and below the threshold limits of sediment quality guidelines.

Keywords Hydrocarbons · PAHs · Sediment cores · Patos Lagoon estuary · Mud bank

Introduction

Coastal zones are the receptors of many substances from natural processes and human activities (Naidu et al., 2021), ranging from organic matter to complex mixtures of synthetic organic and inorganic contaminants. As population density and economic activity in coastal regions increase, these environments are vulnerable to anthropogenic inputs that may lead to concerning levels of environmental contamination (Cabral et al., 2019). Among the most relevant and ubiquitous contaminant groups, hydrocarbons (HCs) are chemical markers of land-based organic inputs (Lu et al., 2022; Volkman et al., 1992). Due to their partition coefficients, HCs preferentially accumulate in the particulate phases (Santos et al., 2023), making sediments the most suitable matrix for spatial and temporal studies.

In aquatic environments, HCs are commonly found as complex mixtures derived from numerous overlapping sources and are potentially deleterious to the environment (Goswami et al., 2016; Ramzi et al., 2017). The relative concentrations of aliphatic (AHs) and polycyclic aromatic (PAHs) hydrocarbons in sediments have been used to distinguish among different hydrocarbon sources (petrogenic, pyrogenic, biogenic, and diagenetic). AHs are a major component of petroleum and its derivatives, although they can also be synthesized by algae and higher plants (Kumar et al., 2016; Meyers, 1997; Volkman et al., 1992). PAHs are mostly derived from anthropogenic sources, specifically the incomplete combustion of organic matter (fossil fuel and wood) and the spillage of petroleum and its byproducts (Chen & Chen, 2011; Readman et al., 2002; Zhang et al., 2015).

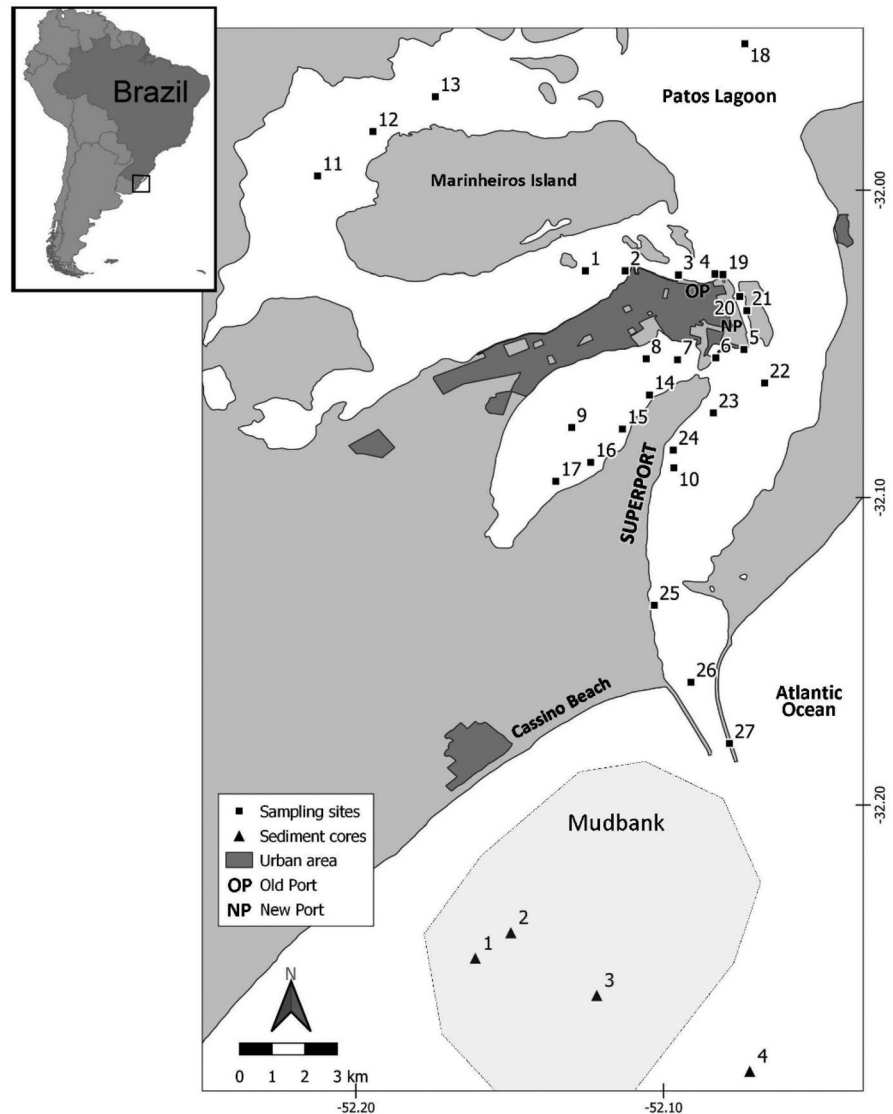
Estuaries are important transition zones between fluvial and marine systems that can act as temporary or permanent traps for anthropogenic contaminants. The sediment balance between inputs of terrestrial or adjacent coastal zones and outputs relies on the local hydrodynamics of tides, waves, and river flows (Zou

et al., 2016). Since many contaminants may adversely affect estuarine and coastal ecosystems, it is important to increase knowledge of their distribution, concentration, transference processes, and impacts (Wu et al., 2023).

The Patos Lagoon (PL), located on the southern Brazilian coast (30–32°S), is the world's largest choked coastal lagoon (Bueno et al., 2021) (Fig. 1). The estuarine region, which covers approximately 10% of the total area, has great economic and ecological importance due to its high productivity (Seeliger, 2001). This area, however, has been subject to intense anthropogenic pressure related to maritime (Rio Grande port complex is the second largest in Brazil), industrial (oil refinery, fertilizers plants, food industries, etc.), and urban activities (the cities of Rio Grande and São José do Norte used to discard untreated sewage into the estuarine waters) (Wallner-Kersanach et al., 2016). Its riverine tributaries, running off organic matter from extensive natural grasslands (Boldrini & Eggers, 1996), provide a large amount of fine sediments to the PL system. According to the hydrodynamics, these fine materials can be trapped in the estuary or carried out to the adjacent coastal areas (Burchard et al., 2018). As a result, a large mud deposit (mud bank) has formed south of Patos Lagoon output (offshore Cassino Beach), mostly between the 6 and 20-m isobaths (Holland et al., 2009) (Fig. 1). During severe storm events, mud bank sediments can be remobilized and transported to the shoreface and/or beach (Calliari et al., 2001), which could potentially be linked to dredging operations in Rio Grande port. However, this is still a controversial topic (Garcia et al., 2021). As fine sediments can adsorb and accumulate contaminants, local biota and beach users at Cassino Beach might be under threat.

Previous studies have shown moderate to high concentrations of hydrocarbons in estuarine sediments near the main sources of contamination (domestic/industrial sewages and harbor activities) (Garcia et al., 2010; Medeiros et al., 2005). However, neither the processes of transference of hydrocarbons from the estuarine system to the adjacent coast nor their levels in the adjacent coastal depositional areas have been previously appraised. Thus, the present study assessed the levels and sources of hydrocarbons to address evidence of processes of transport and degradation of these compounds from the estuary to the adjacent coastal mud bank. Levels and sources of HCs were discussed in the

Fig. 1 Study area (with the mud bank location obtained from Holland et al., 2009) and sampling sites: ■— surface samples inside the Patos Lagoon estuary and —sediment cores at the Cassino Beach mud bank



face of the estuarine morphology and depositional aspects of the mud bank.

Methodology

Sampling

Superficial sediment samples (top 2 cm) were collected inside the Patos Lagoon estuary using a stainless-steel grab and stored in precleaned aluminum containers (-15°C) until analysis. Sediment samples from the

shallow areas and/or nearby potential anthropic sources (sites 1 to 17) were collected once in September 2003 ($N=1$), while samples from the main navigation channel (sites 18 to 27) were collected five times (January and July 2006 and April, June, and October 2007; $N=5$) (Fig. 1). In addition, four sediment cores were collected in November 2005 by scuba diving in the mud bank located in front of Cassino beach (Fig. 1) (Vinzón et al., 2009). The locations and descriptions of the sampling sites are available in Table S1 of the Supporting Information. In the laboratory, cores were sliced into 2-cm layers to obtain interposed samples for grain size analysis,

total organic carbon (TOC), age dating, and hydrocarbon determinations. Samples were placed in precleaned aluminum containers and stored at $-15\text{ }^{\circ}\text{C}$ until analyses.

Analysis

Bulk parameters

Sedimentation rates and sediment radiochronology were determined based on the relative concentrations of ^{210}Pb and/or ^{137}Cs , as described by Reed et al. (2009). TOC was determined using a CHNS Perkin-Elmer 2400 Serie II, according to Yang et al. (1998). Grain size and sediment density analyses were performed as described by Gray and Elliott (2014).

Analysis of hydrocarbons

All samples were freeze-dried, grounded, and analyzed as described by Niencheski and Fillmann (2006) within 1 year of sampling. Briefly, 15 g of dried sediments were spiked with surrogate standards (1-hexadecene and 1-eicosene, and *p*-Terphenyl- D_{14}) and Soxhlet-extracted for 12 h with *n*-hexane/dichloromethane (1:1) after stabilization (2 h). Activated copper was added to remove sulfur. Extracts were concentrated ($\sim 1\text{ mL}$) and cleaned up and fractionated using a column of silica gel (6 g, deactivated with 5% water) and neutral aluminum oxide (8 g, deactivated with 5% water). Elution was performed using 25 mL of hexane to yield the first fraction (which contains the AHs—F1), followed by 30 mL of *n*-hexane/dichloromethane (90:10) and 25 mL of *n*-hexane/dichloromethane (50:50) (which combined contain the PAHs—F2). Fractions F1 and F2 were concentrated, transferred to vials, and fortified with internal standards for AHs (1—tetradecene) and PAHs (naphthalene- d_8 , acenaphthene- d_{10} , phenanthrene- d_{10} , chrysene- d_{12} , perylene- d_{12}), respectively. The final volume was adjusted to exactly 1 mL using N_2 , and an aliquot of 1 μL of each extract was analyzed by GC-FID (F1) and GC-MS (F2). AHs concentrations were not determined for sites 18 to 27, since these sites were originally used exclusively to assess the PAHs levels associated with activities at Rio Grande port.

AHs (F1) were analyzed on a Perkin Elmer Clarus 500 gas chromatograph equipped with a flame ionization detector (GC-FID), an autoinjector, and an

Elite-1 capillary column (100% dimethylpolysiloxane; $30\text{ m}\times 0.25\text{ mm}\times 0.25\text{ }\mu\text{m}$ film thickness). Helium was used as the carrier gas (1.5 mL min^{-1}). The injector temperature was maintained at $280\text{ }^{\circ}\text{C}$ in splitless mode, while the GC temperature was programmed from $40\text{ }^{\circ}\text{C}$ to $290\text{ }^{\circ}\text{C}$ at $5\text{ }^{\circ}\text{C min}^{-1}$, maintained at $290\text{ }^{\circ}\text{C}$ for 10 min, increased to $300\text{ }^{\circ}\text{C}$ at $10\text{ }^{\circ}\text{C min}^{-1}$, and then held at $300\text{ }^{\circ}\text{C}$ for 10 min.

PAHs analyses were carried out using a gas chromatograph equipped with a mass spectrometer detector (Perkin Elmer Clarus 500—GC-MS) and an Elite-5MS silica capillary column (5% phenyl-95% methylpolysiloxane; $30\text{ m}\times 0.25\text{ mm}$, $0.25\text{ }\mu\text{m}$ film thickness). The injector was kept at $280\text{ }^{\circ}\text{C}$ in splitless mode. The GC temperature was programmed from 40 to $60\text{ }^{\circ}\text{C}$ at $10\text{ }^{\circ}\text{C min}^{-1}$, from 60 to $290\text{ }^{\circ}\text{C}$ at $5\text{ }^{\circ}\text{C min}^{-1}$, maintained at $290\text{ }^{\circ}\text{C}$ for 5 min, increased to $300\text{ }^{\circ}\text{C}$ at $10\text{ }^{\circ}\text{C min}^{-1}$, and then held at $300\text{ }^{\circ}\text{C}$ for 10 min. Helium was used as the carrier gas (1.5 mL min^{-1}). Ion source and transfer line temperatures were set at $290\text{ }^{\circ}\text{C}$, and 70 eV was used for ionization. Selected ion monitoring mode was used for quantification. Data acquisition was performed in SIFI (Selected Ion and Full Ion Scanning).

Compound identification was based on individual mass spectra and GC retention times in comparison to library data and authentic standards (Supelco). Instrumental calibration was performed for 23 PAHs with solutions containing naphthalene (Nap), 2-methylnaphthalene (2-MN), 1-methylnaphthalene (1-MN), 1,7-dimethylnaphthalene (1,7-DMN) and 2,6-dimethylnaphthalene (2,6-DMN), acenaphthylene (Acy), acenaphthene (Ace), fluorene (Fl), phenanthrene (Phe), methylphenanthrene (C1Phe), anthracene (Ant), fluoranthene (Flu), pyrene (Pyr), benz[a]anthracene (BaA), chrysene (Chr), benzo[b]fluoranthene (BbF), benzo[k]fluoranthene (BkF), benzo[a]pyrene (BaP), indeno[1,2,3-cd]pyrene (InP), dibenz[a,h]anthracene (DBA), benzo[ghi]perylene (BP), benzo[e]pyrene (BeP), and perylene (Per) at different concentrations (5, 10, 20, 50, 100, 250, and 500 ng mL^{-1}). For AHs, the calibration was made with *n*- C_{12-36} , pristane, and phytane at 0.5, 1, 2, 4, 8, 12, 15, 20, 25, and $50\text{ }\mu\text{g mL}^{-1}$. Compound quantitation was performed using the following internal standards: 1-tetradecene (for AHs), naphthalene- d_8 , acenaphthene- d_{10} , phenanthrene- d_{10} , chrysene- d_{12} , and perylene- d_{12} (for PAHs).

Quality assurance and quality control were based on regular analyses of blanks, spiked matrices, and certified reference material (IAEA-417). Recoveries

for surrogate standards varied between 40 and 100%, while for CRM-IAEA-417, they were between 70 and 112% ($n=10$) (Table S2). Limits of quantitation (LOQ) were the lowest quantifiable concentration of the calibration curve (0.3 ng g^{-1} for PAHs and $0.03 \text{ } \mu\text{g g}^{-1}$ for AHs). During the period of these analyses (2005–2008), our Laboratory (CONECO—FURG; <https://coneco.furg.br>) was certified by the Canadian Association for Laboratory Accreditation (www.cala.ca) for PAH analysis in sediment samples.

Hydrocarbons data analysis

The sources of *n*-alkanes were assessed by applying selected diagnostic ratios. The CPI (carbon preference index, $n\text{-C}_{24}\text{-}n\text{-C}_{35}$) was calculated to further verify the predominant source of *n*-alkanes. According to Bi et al. (2005), CPI values above 2.3 suggest the predominance of higher plants, while CPI values close to 1 usually imply the predominance of anthropogenic *n*-alkanes derived from oil contamination (Keshavarzifard et al., 2020). However, some studies suggest that a CPI below 1.5 can also indicate planktonic inputs as the main source of *n*-alkanes (Bakhtiari et al., 2011). The terrigenous/aquatic ratio (TAR) evaluates the terrigenous inputs versus aquatic inputs $([n\text{-C}_{27}] + [n\text{-C}_{29}] + [n\text{-C}_{31}]) / ([n\text{-C}_{15}] + [n\text{-C}_{17}] + [n\text{-C}_{19}])$, where values above 1.0 correspond to terrigenous material (Vaezzadeh et al., 2015). The proxy P_{aq} (aquatic macrophytes/emergent and terrestrial species) uses the relative proportion of mid-chain to long-chain homologs (Ankit et al., 2017). $P_{\text{aq}} < 0.1$ corresponds to terrestrial plants, 0.1–0.4 to mixed sources, and > 0.4 –1 to submerged/floating macrophytes.

Molecular indexes (ratios between specific PAHs) can be used to assess the sources of PAHs introduced into the environment, considering their thermodynamic characteristics and the proportions of compounds found in the emissions sources and sediments (Goswami et al., 2016; Ramzi et al., 2017; Yunker et al., 2002). Thus, four indexes were applied, according to Yunker et al. (2002): Benzo[a]anthracene/benzo[a]anthracene+chrysene ratio (BaA/(BaA+CHR)) helps to distinguish between inputs of oil (< 0.2), combustion (> 0.35), and the mixture between the former, while the anthracene/anthracene+phenanthrene ratio (ANT/(ANT+PHE)) differentiates between petrogenic (< 0.1), fossil fuel combustion (0.1–0.2) and combustion (> 0.2) inputs. For the fluoranthene/

fluoranthene+pyrene ratio (FLU/(FLU+PYR)), values of > 0.5 indicate grass, wood, and coal combustion, values between 0.5 and 0.4 indicate combustion of fossil fuels, and values < 0.4 are indicative of oil inputs. The indeno[1,2,3-c,d]pyrene/indeno[1,2,3-c,d]pyrene+benzo[ghi]perylene ratio (ID/(ID+BPER)) differentiates between petrogenic (< 0.2), fossil fuel combustion (0.2 and 0.5) and grass, wood, and coal combustion inputs (> 0.5). Spearman's correlation was also calculated between hydrocarbon concentrations, grain size, and TOC.

Results and discussion

AHs and PAHs results for the Patos Lagoon estuary are shown in Table 1, while the Cassino Beach mud bank samples are shown in Table 2.

Hydrocarbons in superficial sediments

Aliphatic hydrocarbons

Concentrations of total aliphatic hydrocarbons (total AHs)—comprehending the resolved aliphatic fraction plus the unresolved complex mixture (UCM)—in superficial sediments varied from 0.68 to $3383 \text{ } \mu\text{g g}^{-1}$ dry weight (d.w.) inside the estuary and 20.3 to $36.0 \text{ } \mu\text{g g}^{-1}$ d.w. in the mud bank (Tables 1 and 2, and Fig. 2). The highest values were found nearby the possible anthropogenic sources, while the lowest were in the main navigation channel and areas further away from the possible direct sources (Fig. S1). According to Volkman et al. (1992), total AHs concentrations above $100 \text{ } \mu\text{g g}^{-1}$ are generally associated with oil inputs to the environment, and values above $500 \text{ } \mu\text{g g}^{-1}$ are indicative of chronic hydrocarbon contamination. Considering these thresholds, sites 2 (marina), 3 (city market), and 4 (dry docking) were likely contaminated by oil inputs, while sites 6 (Sewage), 7 (petroleum distributor), and 8 (petroleum refinery) were chronically contaminated. The total AHs concentrations were below $10 \text{ } \mu\text{g g}^{-1}$ at sites 1 (Pombas Island), 11, 12, 13 (Marinheiros Island), 14, 16, and 17 (Mangueira Cove). Such values (and even higher in areas with significant biogenic inputs) are similar to concentrations reported for areas considered to be free of contamination (Dauner et al., 2015; Readman et al., 2002; Volkman et al., 1992).

Table 1 Concentrations of total aliphatic hydrocarbons (AHs), sum of alkanes, UCM, Σ_{23} PAHs, total organic carbon, fine sediments, and selected diagnostic ratios for the sediments sampled in the Patos Lagoon estuary. Results shown for sites 18 to 27 are derived from 5 sampling events (average \pm standard deviation; $N=5$), while all others are based on a single sampling ($N=1$)

Station	Total AHs ($\mu\text{g g}^{-1}$)	$\Sigma n\text{C}_{12-36}$ ($\mu\text{g g}^{-1}$)	UCM ($\mu\text{g g}^{-1}$)	UCM/RA	UCM (%)	TAR	ACL	P_{aq}	CPI	alk _{terr} (%)	Σ_{23} PAHs (ng g^{-1})	%PER/5-ringPAH	LMW/HMW	FLU/FLU + PYR	ANT/ANT + PHE	ID/ID + BPER	BaA/BaA + CHR	TOC (%)	Fine sediments (%)
1	0.75	0.46	<LOQ	n.c.	n.c.	0.19	28.4	0.20	1.6	12.1	30.1	21.2	3.7	0.54	n.c.	0.6	0.36	0.3	2.7
2	206.6	6.0	186.1	9.1	90.0	2.7	28.5	0.15	4.5	49.1	869.1	16.0	0.55	0.55	0.9	n.c.	0.42	1.7	50.5
3	261.5	17.9	218.3	5.1	83.5	0.63	27.8	0.28	2.1	20.9	305.4	51.6	1.2	0.47	0.49	0.5	0.32	2.1	89.8
4	355.0	4.01	329.1	56.0	92.7	2.1	28.3	0.21	2.8	37.6	2303.3	11.7	0.61	0.56	0.68	0.58	0.42	1.3	48.6
5	52.6	1.8	47.7	9.7	90.6	4.1	28.3	0.21	3.7	52.9	879.6	16.0	3.9	0.59	0.99	n.c.	0.59	0.79	37.4
6	573.1	36.4	501.9	7.1	87.6	2.9	28.1	0.21	1.8	38.9	388.6	42.0	0.52	0.48	0.3	0.53	0.33	3.5	95.5
7	1388.4	2.29	1377.4	124.3	99.2	2.1	28.4	0.19	2.6	42.6	329.0	6.5	0.09	0.28	n.c.	0.01	0.16	1.2	30.2
8	3383.6	7.12	3353.1	109.9	99.1	1.6	28.6	0.18	2.7	36.4	577.8	28.0	0.34	0.44	0.59	0.44	0.22	2.4	88.0
9	16.5	1.6	12.6	3.3	76.7	4.3	28.4	0.20	3.3	49.0.4	44.8	60.0	0.55	0.51	n.c.	0.48	0.19	0.79	28.4
10	23.95	0.75	21.1	7.4	88.2	4.1	28.0	0.25	2.9	42.5	151.9	22.8	0.41	0.54	n.c.	0.5	0.31	0.93	40.1
11	1.1	0.53	<LOQ	n.c.	n.c.	0.51	28.4	0.18	1.4	22.8	2.4	56.7	0.76	0.58	n.c.	0.6	0.07	0.28	5.3
12	0.91	0.44	<LOQ	n.c.	n.c.	0.33	28.9	0.14	1.4	19.2	2.0	65.7	1.0	n.c.	n.c.	n.c.	n.c.	0.29	3.9
13	0.68	0.38	<LOQ	n.c.	n.c.	0.54	27.9	0.28	1.6	21.3	4.0	52.6	0.91	0.6	n.c.	0.6	0.12	0.31	9.1
14	14.4	0.63	12.8	8.1	89.0	7.2	28.0	0.23	2.1	43.5	9.3	77.9	10.6	0.47	n.c.	0.5	0.16	0.41	5.7
15	15.8	0.88	13.8	7.0	87.4	2.5	28.3	0.19	6.0	52.4	5.4	54.4	0.43	0.51	n.c.	0.4	0.25	0.62	4.6
16	1.7	0.45	<LOQ	n.c.	n.c.	0.56	28.1	0.24	3.3	28.2	9.8	4.7	0.10	0.43	n.c.	0.31	0.38	0.28	0.0
17	0.70	0.28	<LOQ	n.c.	n.c.	3.0	29.7	0.11	2.4	43.8	0.5	n.c.	0.00	n.c.	n.c.	n.c.	n.c.	0.28	0.0
18	Data not available																		
19											122.2 \pm 31.4	83.4	0.56	0.6	0.20	n.c.	0.49	Data not available	
20											56.7 \pm 43.2	72.0	0.91	0.56	0.22	n.c.	0.52		
21											148.8 \pm 18.7	77.6	0.49	0.57	0.17	n.c.	0.54		
22											165.1 \pm 157.5	70.6	0.50	0.56	0.19	n.c.	0.55		
23											96.2 \pm 20.1	81.5	0.61	0.57	0.18	n.c.	0.52		
24											89.8 \pm 34.9	73.7	0.58	0.57	n.c.	n.c.	0.56		
25											142.2 \pm 31.8	80.3	0.45	0.58	0.19	n.c.	0.51		
26											182.4 \pm 116.1	65.9	0.49	0.58	0.15	n.c.	0.58		
27											59.1 \pm 45.6	88.6	1.9	0.57	n.c.	n.c.	n.c.		
											81.7 \pm 55.9	76.4	2.6	0.54	0.35	n.c.	0.80		

< LOQ below the quantitation limit, n.c. not calculated, $\Sigma n\text{-C}_{12-36}$ sum of $n\text{-C}_{12}$ to $n\text{-C}_{36}$, UCM Unresolved Complex Mixture, UCM/RA UCM/Resolved aliphatics, TAR $(n\text{-C}_{27} + n\text{-C}_{29} + n\text{-C}_{31}) / (n\text{-C}_{15} + n\text{-C}_{17} + n\text{-C}_{19})$, ACL $(23^*n\text{-C}_{23}) + (25^*n\text{-C}_{25}) + (27^*n\text{-C}_{27}) + (29^*n\text{-C}_{29}) + (31^*n\text{-C}_{31}) / (n\text{-C}_{23} + n\text{-C}_{25} + n\text{-C}_{27} + n\text{-C}_{29} + n\text{-C}_{31})$, P_{aq} $(n\text{-C}_{23} + n\text{-C}_{25} + n\text{-C}_{27} + n\text{-C}_{29} + n\text{-C}_{31}) / (n\text{-C}_{15} + n\text{-C}_{17} + n\text{-C}_{19})$, CPI $(0.5^*(\Sigma \text{odd } n\text{-C}_{25} - n\text{-C}_{33}) / \Sigma \text{even } n\text{-C}_{24} - n\text{-C}_{32}) + (\Sigma \text{odd } n\text{-C}_{25} - n\text{-C}_{33}) / \Sigma \text{even } n\text{-C}_{26} - n\text{-C}_{34})$, alk_{terr} percentage of $n\text{-C}_{27}$, $n\text{-C}_{29}$, $n\text{-C}_{31}$, and $n\text{-C}_{33}$ in relation to $\Sigma n\text{-C}_{12} - n\text{-C}_{36}$, Σ_{23} PAHs sum of 23 PAHs, PER perylene, LMW/HMW low molecular weight/high molecular weight PAHs, FLU fluoranthene, PYR pyrene, ANT anthracene, PHE phenanthrene, ID Indeno[123]pyrene, BPER benzo[ghi]perylene, BaA benzo[a]anthracene, CHR chrysene, TOC total organic carbon

Table 2 Concentrations of total aliphatic hydrocarbons (AHs), sum of alkanes, UCM, Σ_{23} PAHs, total organic carbon, fine sediments, and selected diagnostic ratios for the sediments sampled in the Cassino beach mud bank

Depth (cm)	Total AHs ($\mu\text{g g}^{-1}$)	ΣC_{12-36} ($\mu\text{g g}^{-1}$)	UCM ($\mu\text{g g}^{-1}$)	UCM/RA	UCM (%)	TAR	ACL	P _{aq}	CPI	Alkterr (%)	Σ_{23} PAHs (ng g^{-1})	%PER/5-ringPAH	LMW/HMW	FLU/FLU+Pyr	ANT/ANT+PHE	ID/ID+BPER	BaA/BaA+CHR	TOC (%)	Fine sediments (%)
Core 1	2.5–5	20.3	0.81	15.4	3.1	75.5	n.c.	29.0	0.12	3.7	66.7	15.2	80.1	0.35	0.53	0.53	0.41	0.89	60.0
	17.5–21	29.3	1.3	23.1	3.7	78.7	n.c.	28.4	0.21	2.7	56.4	15.1	72.9	0.27	0.51	0.52	0.38	0.85	73.5
	34–37	25.5	1.1	19.5	3.3	76.6	n.c.	28.3	0.22	2.2	52.9	7.6	72.4	0.37	0.51	n.c.	n.c.	0.48	70.8
	43.5–45	22.3	0.93	16.2	2.7	72.9	n.c.	27.9	0.28	1.9	47.5	14.4	79.9	0.28	0.51	0.53	0.46	0.50	n.a
	60–62	32.2	1.3	23.6	2.7	73.2	n.c.	28.7	0.18	3.3	61.4	33.4	80.5	0.28	0.52	0.50	0.43	1.0	72.7
Core 2	0–3	21.4	0.07	11.5	0.87	53.8	n.c.	30.0	n.c.	n.c.	100.0	0.85	100.0	n.c.	n.c.	n.c.	n.c.	0.26	27.1
	10–13	11.6	<LOQ	9.4	4.2	80.9	n.c.	n.c.	n.c.	n.c.	<LOQ	n.c.	n.c.	n.c.	n.c.	n.c.	n.c.	0.09	33.3
	20–23	29.5	1.5	22.3	3.0	75.4	n.c.	28.8	0.14	3.6	64.67	17.4	77.6	0.33	0.56	n.c.	0.37	1.1	72.2
	30–33	18.6	0.95	12.9	2.3	69.4	n.c.	28.9	0.14	2.2	56.9	8.3	83.4	0.68	0.57	n.c.	n.c.	0.51	18.5
	40–43	21.4	1.7	13.2	1.6	61.6	n.c.	28.1	0.23	1.7	48.3	18.5	81.8	0.48	0.54	n.c.	0.38	1.3	67.3
Core 3	50–53	31.2	0.79	13.0	0.71	41.4	n.c.	28.2	0.20	1.4	46.8	6.3	82.5	0.38	0.55	n.c.	n.c.	0.39	87.2
	60–63	18.4	0.96	13.1	2.5	71.0	n.c.	28.3	0.23	2.2	53.0	10.7	88.2	0.33	0.58	n.c.	n.c.	0.61	51.9
	0–2	36.0	1.7	28.8	4.1	80.1	n.c.	28.6	0.18	3.1	58.1	119.5	87.9	0.55	0.53	0.49	0.38	1.5	99.6
	6–8	26.3	1.2	21.3	4.2	80.9	n.c.	28.5	0.19	3.2	60.9	69.2	75.7	0.59	0.51	0.53	0.41	1.2	95.2
	16–18	27.3	1.7	20.6	3.1	75.4	n.c.	28.4	0.20	3.0	57.8	98.0	81.4	0.47	0.55	0.59	0.38	1.3	97.1
Core 4	23–30	31.5	1.9	24.2	3.3	76.9	n.c.	28.5	0.19	3.4	59.9	97.6	75.6	0.42	0.55	0.53	0.38	1.5	99.3
	33–40	31.2	2.8	27.6	2.5	88.5	n.c.	28.4	0.20	2.5	54.1	106.2	77.6	0.41	0.57	0.54	0.37	1.6	100.0
	43–50	34.2	1.4	19.6	3.2	57.2	n.c.	28.6	0.17	3.2	61.5	69.5	76.4	0.46	0.54	0.52	0.37	1.2	99.8
	53–60	31.7	2.0	26.0	3.2	82.0	n.c.	28.6	0.17	2.9	59.4	93.9	72.3	0.36	0.52	0.52	0.39	1.4	90.2
	0–2	29.7	1.7	22.6	4.1	76.2	n.c.	28.7	0.17	3.5	62.0	14.5	80.6	0.29	0.54	0.57	0.41	1.3	n.a
Core 4	6–10	26.3	1.9	18.9	4.2	71.7	n.c.	28.5	0.18	2.2	54.7	12.6	75.3	0.38	0.55	0.50	0.40	0.89	65.0
	13–20	22.8	0.67	18.9	3.1	82.8	n.c.	28.9	0.13	2.9	62.1	7.1	78.4	0.58	0.55	n.c.	n.c.	0.91	80.3
	23–30	30.6	1.7	22.9	3.3	74.9	n.c.	28.4	0.20	2.4	54.7	12.6	70.8	0.33	0.53	0.58	0.40	1.2	80.1
	33–40	29.5	0.76	25.2	2.5	85.5	n.c.	29.0	0.11	3.5	67.0	8.7	69.5	0.44	0.53	n.c.	0.41	0.90	70.2
	45–50	32.5	1.2	26.8	3.2	82.4	n.c.	28.8	0.15	3.6	64.3	11.8	72.5	0.28	0.49	0.52	0.40	1.1	78.5
53–60	31.8	1.6	24.1	3.2	75.7	n.c.	n.c.	28.3	0.21	1.9	50.4	17.5	67.5	0.26	0.50	0.53	0.41	0.86	93.7

< LOQ below the quantitation limit, n.c. not calculated, $\Sigma n\text{-C}_{12-36}$ sum of n-alkanes $n\text{-C}_{12}$ to $n\text{-C}_{36}$, UCM Unresolved Complex Mixture, UCM (%)/UCM*100/Total AHs, UCM/RA UCM/Resolved aliphatics, TAR $(n\text{-C}_{27} + n\text{-C}_{29} + n\text{-C}_{31})/(n\text{-C}_{15} + n\text{-C}_{17} + n\text{-C}_{19})$, ACL $((23*n\text{-C}_{25}) + (27*n\text{-C}_{27}) + (29*n\text{-C}_{29}) + (31*n\text{-C}_{31}))/((n\text{-C}_{23} + n\text{-C}_{25} + n\text{-C}_{27} + n\text{-C}_{29} + n\text{-C}_{31}))$, P_{aq} $(n\text{-C}_{23} + n\text{-C}_{25})/(n\text{-C}_{23} + n\text{-C}_{25} + n\text{-C}_{27} + n\text{-C}_{29} + n\text{-C}_{31})$, CPI $(n\text{-C}_{25} + n\text{-C}_{27})/(n\text{-C}_{23} + n\text{-C}_{25})$, Σ_{23} PAHs sum of 23 PAHs, PER perylene, LMW/HMW low molecular weight/high molecular weight PAHs, FLU fluoranthene, PYR pyrene, ANT anthracene PHE phenanthrene, ID Indeno[123]pyrene, BPER Benzo[ghi]perylene, BaA benzo[a]anthracene, CHR chrysene, TOC total organic carbon

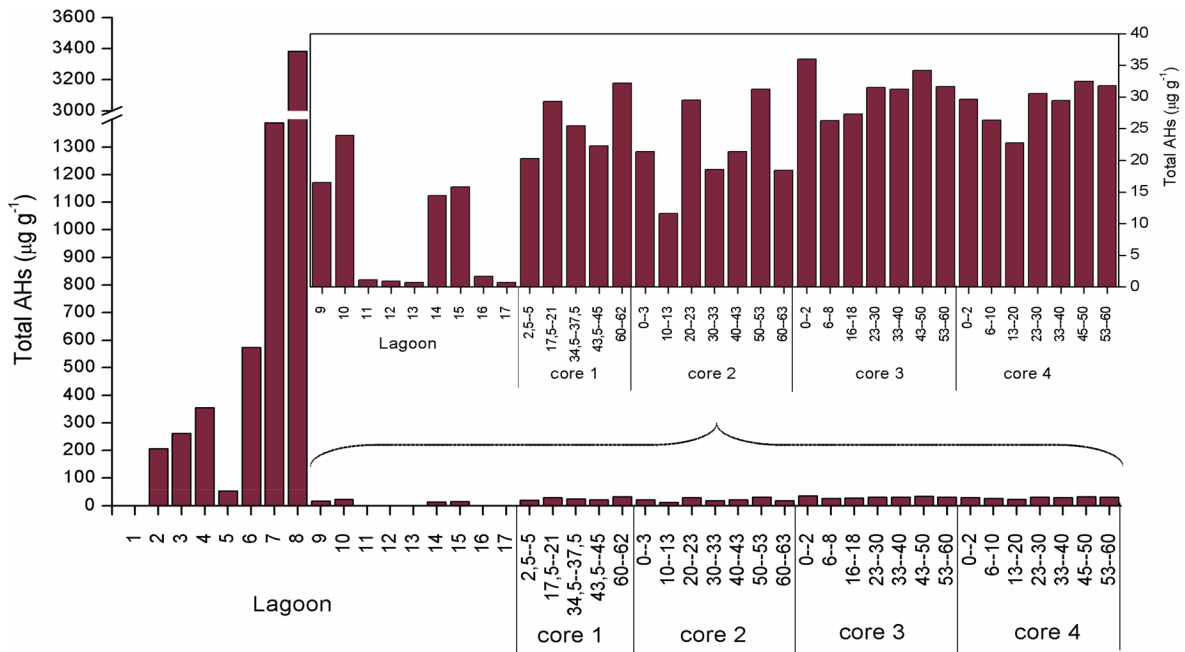


Fig. 2 Total aliphatic hydrocarbons concentration ($\mu\text{g g}^{-1}$) in surface sediments sampled inside the Patos Lagoon estuary and in the sediment cores collected in the Cassino beach mud bank. Aliphatic hydrocarbons were not analyzed at sites 18 to 27

No correlation was observed between total AHs concentrations and grain size ($p > 0.05$) or between total AHs and TOC ($p > 0.05$).

UCM concentrations in superficial sediments varied between $<\text{LOQ}$ and $3353 \mu\text{g g}^{-1}$ (d.w.) (estuary) and 11.5 and $28.8 \mu\text{g g}^{-1}$ (d.w.) (mud bank) (Tables 1

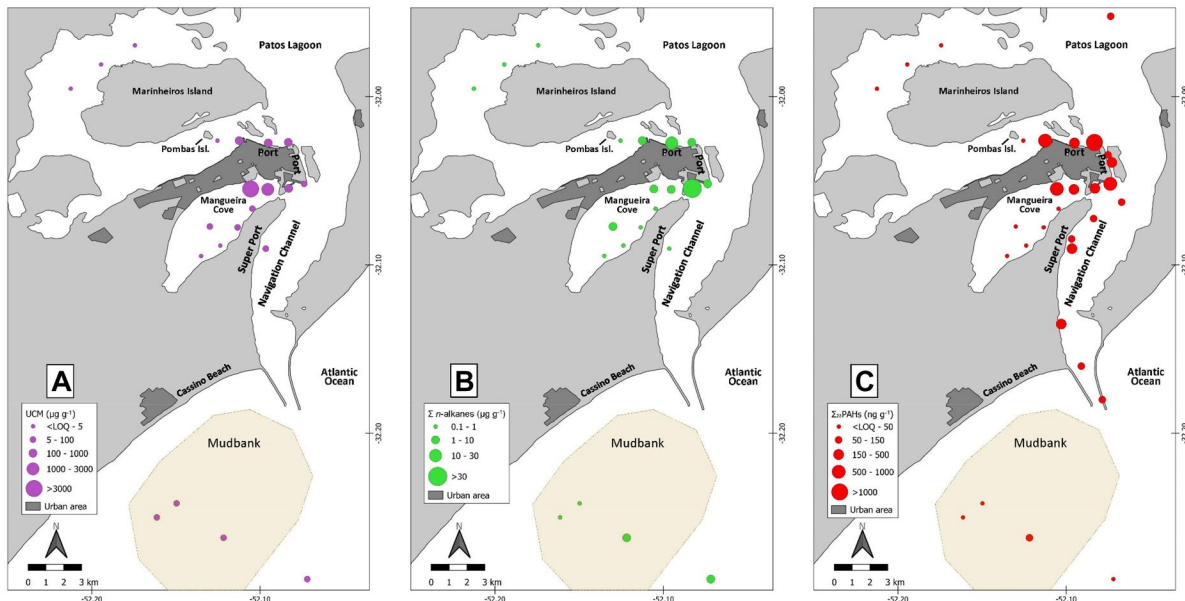


Fig. 3 Spatial distribution of **a** UCM concentrations ($\mu\text{g g}^{-1}$), **b** alkanes (sum of $n\text{-C}_{12-36}$) concentrations ($\mu\text{g g}^{-1}$), and **c** $\Sigma_{23}\text{PAHs}$ concentrations (ng g^{-1}) in surface sediments sam-

pled inside the Patos Lagoon estuary and in the sediment cores collected in the Cassino beach mud bank. Aliphatic hydrocarbons were not analyzed at sites 18 to 27

and 2, and Fig. 3a). The presence of UCM is generally associated with degraded or weathered oil residues (Readman et al., 2002; White et al., 2013), being formed by resistant molecules that tend to accumulate in the sediment. UCM was present in 76% of the stations, representing 54 to 99% of the total AHs (Table 1). High levels of total AHs and predominance of UCM suggest chronic oil input at sites 2 (marina), 3 (city market), 4 (dry docking), 6 (sewage), 7 (petroleum distributor), and 8 (petroleum refinery). Additional evidence of chronic oil introduction is provided by the ratio between UCM and resolved aliphatic hydrocarbons, with results above 4 indicating contributions of degraded oil products (Yunker et al., 2002). Most sites showed results above 4, and very high ratios were observed at sites 4 (56), 7 (124), and 8 (110) (Table 1), while the ratio was 0 at sites 10, 11, 12, 13, 15, and 16 (Table 1). Despite the UCM predominance at sites 5 (Fertilizer industry), 10 (Oil Terminal), 14 (Mangueira Cove 2), and 15 (Mangueira Cove 3), total AHs levels were low and similar to those found in non-contaminated areas (Massone et al., 2013; Medeiros & Bicego, 2004).

The sum of $n\text{-C}_{12-36}$ alkanes in superficial sediments ranged from 0.28 to 36.4 $\mu\text{g g}^{-1}$ (d.w.) (estuary) and 0.07 to 1.7 $\mu\text{g g}^{-1}$ (d.w.) (mud bank) (Tables 1 and 2, and Fig. 3b). Although concentrations of n -alkanes observed in the sediments of the Patos Lagoon estuary slightly were higher than those observed in a previous study (0.2 – 7.5 $\mu\text{g g}^{-1}$; Medeiros et al., 2005), they were on the same order of magnitude as those reported for other locations in Brazil under moderate human impact (6.04 – 44.0 $\mu\text{g g}^{-1}$; Martins et al., 2015; 4.2 – 55.6 $\mu\text{g g}^{-1}$; Assunção et al., 2017). However, they were lower than sites considered heavily impacted, such as Guanabara Bay, Brazil (3.0 – 318 $\mu\text{g g}^{-1}$; Farias et al., 2008) and Malacca Strait, Malaysia (28.0 – 254.5 $\mu\text{g g}^{-1}$; Vaezzadeh et al., 2015). However, remote locations can also present similar levels of n -alkanes when compared to the Patos Lagoon estuary and Cassino Beach mud bank, such as Camamu, Brazil (0.77 – 55.17 $\mu\text{g g}^{-1}$; Paixao et al., 2010) and King George Island, Antarctic, (0.5 – 4.9 $\mu\text{g g}^{-1}$; Dauner et al., 2015).

Individual n -alkane distributions revealed the predominance of odd long-chain n -alkanes ($n\text{-C}_{29}$ and $n\text{-C}_{31}$) at most stations, suggesting a biogenic contribution from terrigenous sources (higher plant waxes)

(Medeiros & Bicego, 2004; Volkman et al., 1992). This is confirmed by the predominance of n -alkanes associated with terrestrial sources (alk_{terr}) at most sites (Table 1). $n\text{-C}_{31}$ showed the highest concentrations at most sites, indicating inputs from C4-type grasses (Bush & McInerney, 2015; Schefuß et al., 2003) from both salt marshes of the Patos Lagoon estuary (e.g., *Spartina alterniflora*, *Spartina densiflora*, etc.) (Marangoni & Costa, 2009) and the run-off of the extensive natural grasslands along the Patos Lagoon drainage basin (Boldrini & Eggers, 1996).

In the present study, most sediments presented CPI ratios above 2.3, suggesting inputs from higher plants (Table 1). CPI ratios, however, were close to 1 at sites 1 (Pombas Island), 11, 12, and 13 (Marinheiros Island). These sites also presented low levels of total AHs and no UCM, suggesting that n -alkanes from planktonic sources were more likely than petrogenic inputs. $n\text{-C}_{17}$ was also observed at most sites, suggesting that planktonic inputs from algal blooms (Chevalier et al., 2015) were another probable source of n -alkanes inside the Lagoon.

Although the terrigenous/aquatic ratio (TAR) ratios varied between 0.19 and 7.23, most sites showed values indicating terrigenous sources, as seen for CPI ratios. Ratios for sites 1 (Pombas Island), 11, 12, and 13 (Marinheiros Island), as also seen for CPI ratios, indicated aquatic inputs. The ratios for sites 3 and 16 also indicated aquatic sources. P_{aq} ratios varied between 0.11 and 0.28, remaining on the mixed sources range and, therefore, showing little differentiation along the sampling area.

The average chain length (ACL) reflects the average number of carbon atoms for n -alkanes (Vaezzadeh et al., 2015). Alkanes $n\text{-C}_{23}$ and $n\text{-C}_{25}$ are associated with *Sphagnum* mosses, $n\text{-C}_{27}$ and $n\text{-C}_{29}$ are related to woody plants, and $n\text{-C}_{31}$ is mostly found in graminoids (grasses). However, the signals of the last two groups may be mixed in the sediments. In the present study, the ACL ranged from 27.8 to 30.0, indicating a mixed source of both woody plants and graminoids.

Polycyclic aromatic hydrocarbons

Total PAHs ($\Sigma_{23}\text{PAH}$) concentrations in superficial sediments ranged from 0.5 to 2303 ng g^{-1} (d.w.)

(estuary) and 0.85 to 119.5 ng g⁻¹ (d.w.) (mud bank) (Tables 1 and 2, and Fig. S2). These results were lower than those previously observed by Medeiros et al. (2005) for the same study area of Patos Lagoon estuary ($\Sigma_{23}\text{PAH}$ —37.7 to 11,780 ng g⁻¹ (d.w.). However, PAH levels were similar to those reported for other locations in Brazil under moderate human impact (15.1 – 1,013 ng g⁻¹, Martins et al., 2015; ng g⁻¹; 26.0 – 434; Assunção et al., 2017), and lower than levels found in heavily contaminated estuaries in Brazil, such as Guanabara Bay (10 – 240,394 ng g⁻¹; Farias et al., 2008) and Fortaleza (3 – 2,235 ng g⁻¹; Cavalcante et al., 2009).

Based on ΣPAH levels, sites can be divided into 3 groups: (i) Highly contaminated—sites 2 (marina), 4 (dry docking), 5 (fertilizer industry), and 8 (petroleum refinery) showed concentrations above 500 ng g⁻¹, characteristic of chronically contaminated environments (Notar et al., 2001); (ii) Moderately contaminated—sites 3 (city market), 6 (sewage), 7 (petroleum distributor), 10 (oil terminal), 18 (São José do Norte), 20 (Rio Grande new port) to 25 (pilot house), 27 (jetty outer edge) and core 3 showed levels above 80 ng g⁻¹; (iii) Low contaminated—sites 1 (Pombas island), 9 (Mangueira cove 1), 11 (Marinheiros island 1) to 17 (Mangueira cove 5), 19 (old port), 26 (inner jetty edge), and cores 1, 2, and 3 (Fig. 3c). As seen for total AHs, no correlation

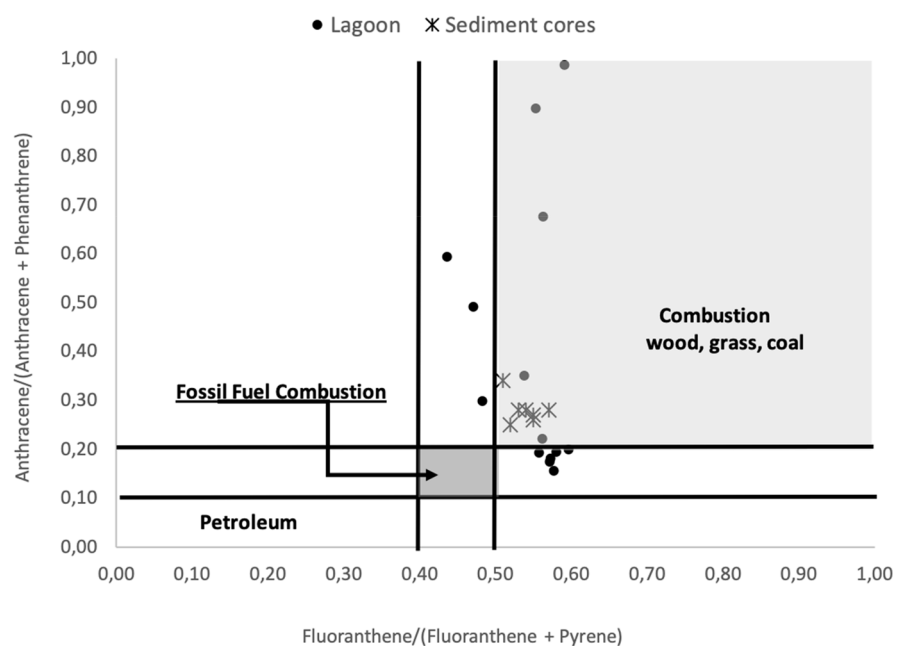
was found between PAHs concentrations vs grain size ($p > 0.05$) and PAHs concentrations vs TOC ($p > 0.05$).

Petrogenic inputs usually have a high proportion of lower molecular weight PAHs (LMW—2 to 3 aromatic rings) and a great abundance of alkylated homologs, while high molecular weight PAHs (HMW—4 to 6 rings) prevail in pyrogenic inputs (Tobiszewski & Namieśnik, 2012). The ratio of HMW/LMW PAHs indicated that HMW PAHs predominated (Table 1), except for sites 1 (Pombas Island), 3 (city market), 5 (fertilizer industry), 14 (Mangueira cove 2), 26 (inner jetty edge), and 27 (outer jetty edge), where LMW PAHs concentrations were higher.

All four PAHs ratios calculated in the present study (BaA/(BaA+CHR), ANT/(ANT+PHE), FLU/(FLU+PYR), and ID/(ID+BPER) indicated the predominance of pyrogenic inputs, specifically wood, grass, or coal combustion (Table 1). This trend can be observed in the cross plot between ANT/(ANT+FEN) and FLU/(FLU+PYR) ratios (Fig. 4). BaA/(BaA+CRI) ratio, however, also indicated petrogenic inputs for some sites, which suggests a mixture of pyrolytic and petrogenic sources to the estuarine sediments (Martins et al., 2011; Yunker et al., 2002).

Perylene is a major diagenetic PAH commonly found in marine sedimentary environments (Silliman et al., 1998). Although its diagenetic precursors are associated

Fig. 4 Cross plot of fluoranthene/(fluoranthene + pyrene) and anthracene/(anthracene + phenanthrene) ratios for surface sediments of Patos Lagoon estuary (■) and Cassino beach mud bank sediment cores (*)



with terrestrial organic matter (Varnosfaderany et al., 2014), pyrogenic processes may yield perylene as well, and such an origin may be dominant in areas receiving high anthropogenic inputs. Its occurrence in levels > 10% of the total penta-aromatic PAHs isomers is attributed to diagenetic sources (Oyo-Ita et al., 2013). In the present study, perylene levels ranged from < LOQ to 130.3 ng g⁻¹ (d.w.) (estuary) and 0.85 to 62.91 ng g⁻¹ (d.w.) (mud bank) and only 2 out of 27 sites (7—petroleum distributor and 16—Mangueira cove 4) showed %PER/5-ring PAH ratios < 10%, suggesting that diagenetic sources prevailed in most of the sampling area.

Sediment quality guidelines are broadly used to assess the contamination of aquatic environments. According to Buchman (2008), TEL (Threshold Effect Level) levels are values below which effects on organisms are rarely expected, while PEL (Probable Effect Level) indicates values above which effects on organisms are frequently expected. All 27 sites showed concentrations of total PAHs below PEL ($\Sigma\text{PAH} < 16,770 \text{ ng g}^{-1}$), while one site (4—dry docking) presented levels above TEL ($\Sigma\text{PAH} > 1,684 \text{ ng g}^{-1}$). In addition, according to the Brazilian guideline (Brasil, 2012), the sum of PAHs should not exceed 4,000 ng g⁻¹ for saline/brackish sediment; therefore, none of the sites surpassed this threshold level.

Sediment cores of the Cassino Beach mud bank

The fine sediments originating inside the Lagoon are transported southward by coastal drift and settle offshore, forming the Cassino beach mud bank (Holland et al., 2009). The mud bank sediments are periodically remobilized and transported to the beach during high-energy events (storms) caused by cold fronts (Calliari et al., 2009). In these situations, the beach can be covered in mud, affecting local tourism and the biota.

Currents and waves modify the mud deposit by transporting and suspending the sediments, influencing the mud density, and classifying the mud by grain size. As wave and current shear forces progressively decrease, the mud finally settles and consolidates (Reed et al., 2009). These processes yield two end-member types of mud: one type that is considered a viscous fluid and another one that is consolidated and can be considered an elastoplastic material (Foda et al., 1993). Usually, the mud type is defined by

the particulates per volume of fluid (g L⁻¹): viscous muds have a density from 10 to 480 g L⁻¹, which corresponds to a density of 1.05 to 1.30 g cm⁻³. In contrast, consolidated mud exceeds this upper limit (Reed et al., 2009).

According to Reed et al. (2009), in cores 2 and 3, the density ranged between 0.73 and 1.53 g cm⁻³ and 1.10 to 1.29 g cm⁻³, respectively, while it ranged from 1.33 to 2.03 g cm⁻³ in core 4 (Table S3). Core 1 was not analyzed. Therefore, cores 2 and 3 consist of fluid mud, while the density is higher in core 4, suggesting consolidated layers. However, the ²¹⁰Pb analyses indicate that all cores presented an initial mixed layer of approximately 40 cm (Reed et al., 2009). The lack of stable layering prevents any temporal analyses of hydrocarbon contamination in the area, and the reconstruction of a depositional history was not possible. Moreover, storm surges may create gaps in the historical registry through sediment remobilization (Figueiredo & Calliari, 2006).

Sediments in the Cassino beach mud bank cores were predominantly fine (silt + clay), in agreement with the results reported for the area (Holland et al., 2009), ranging from 60.0 to 73.5% in core 1, 18.5 to 87.2% in core 2, 90.2 to 100% in core 3, and 65.0 to 93.7% in core 4 (Table 2). Total organic carbon varied between 0.09% and 1.56%, with the highest TOC values found in core 3 (Table 2).

Aliphatic hydrocarbons

Total AHs concentrations were relatively constant throughout all four sediment cores, ranging from 20.3 to 32.2 µg g⁻¹ in core 1, 11.6 to 31.2 µg g⁻¹ in core 2 and 22.8 to 32.5 µg g⁻¹ in core 4, with core 3 showing the highest values (26.3 to 36.0 µg g⁻¹) (Table 2 and Fig. 5).

UCM was present in all analyzed samples and comprised more than 70% of the total AHs in 90% of the samples (Fig. 5). The high abundance of UCM, an indicator of oil contamination (Yunker et al., 2002), suggests a chronic petrogenic input in the area. However, levels were not very high, and the ratio between UCM and resolved aliphatic hydrocarbons (UCM/RA) was > 4 in only 5 samples: core 2 (10–13 cm); core 3 (0–2 cm); core 3 (6–8 cm); core 4 (0–2 cm); and core 4 (6–10 cm), being < 4 in the majority of samples (Table 2). The CPI results were above 1 along all cores and did not suggest petroleum inputs.

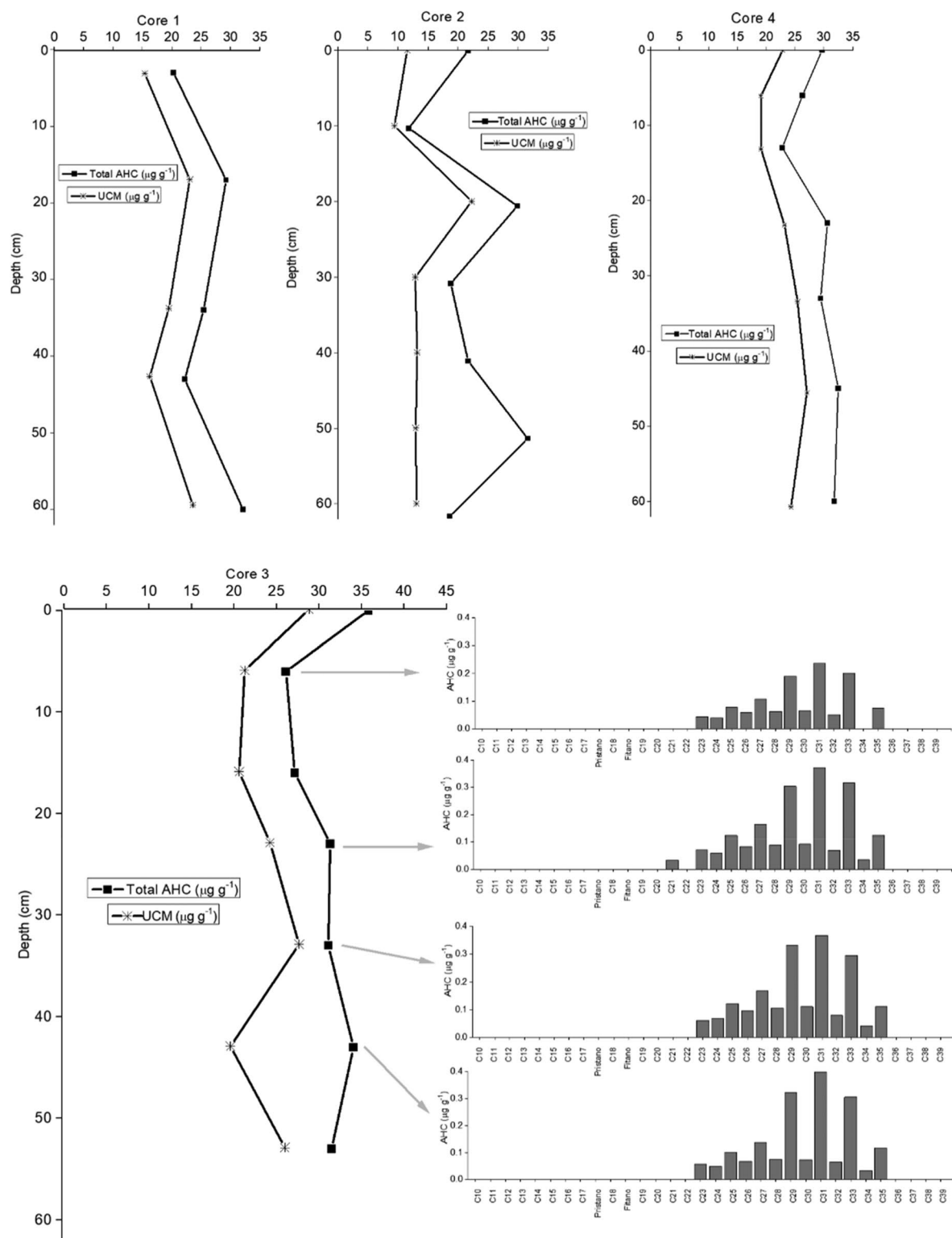


Fig. 5 Sedimentary profile of total AHs and UCM ($\mu\text{g g}^{-1}$) in the Cassino Beach mud bank sediment cores. The individual distribution of alkanes is presented for the selected profile depth of core 3

The $\Sigma n\text{-C}_{12}\text{-}n\text{-C}_{36}$ concentrations were relatively low, ranging from <LOQ to $2.77 \mu\text{g g}^{-1}$. There was no evident trend in *n*-alkane deposition along the cores (Fig. 5). Similar to total AHs, the *n*-alkane concentrations were higher in core 3, with a significant correlation between $\Sigma n\text{-C}_{12}\text{-}n\text{-C}_{36}$ vs TOC ($p < 0.05$) and $\Sigma n\text{-C}_{12}\text{-}n\text{-C}_{36}$ vs fine sediments ($p < 0.05$) in all cores. Individual *n*-alkane distributions revealed the predominance of long-chain odd *n*-alkanes ($C > 23$), indicating input from terrigenous sources. The alk_{ter} ratio results also suggest prominent contributions of higher plants in all cores (Table 2). Similar to the samples collected inside the Lagoon, the $n\text{-C}_{31}$ alkane showed the highest concentrations throughout all sediment cores, indicating the predominance of inputs derived from C4-type grasses (Schefuß et al., 2003). Regarding the other proxies for *n*-alkanes, ACL was similar to the values observed for the estuarine samples, remaining in the range of mixtures of woody and graminoid plants (27.9 – 30.0). The proxy P_{aq} was also like the estuarine area (0.11 – 0.28), pointing out a mixed source range. Additionally, these proxies presented a homogenous distribution along the cores. The TAR values could not be calculated since short-chain *n*-alkanes ($n\text{-C}_{15}$, $n\text{-C}_{17}$, and $n\text{-C}_{19}$) were not detected in any core sediments.

Total AHs and UCM concentrations were relatively constant throughout all four sediment cores, suggesting that either the inputs were constant over time, or the sediment layers were mixed due to physical processes, which is more plausible considering the fluid state of the cores, as explained in the section above. This is also corroborated by the lack of short-chain *n*-alkanes and the high percentage of UCM in the cores. The resuspension and mixing of the sediments make the more labile short-chain *n*-alkanes vulnerable to decomposition, while UCM is more resistant to degradation and is preserved. Therefore, physical processes may influence the record of hydrocarbons stored in mud bank sediments.

Polycyclic aromatic hydrocarbons

The $\Sigma_{23}\text{PAH}$ concentrations varied from 7.6 to 33.4 ng g^{-1} (d.w.) in core 1, <LOQ to 18.5 ng g^{-1} (d.w.) in core 2 and 7.1 to 17.5 ng g^{-1} (d.w.) in core 4, with core 3, as seen for AHs, showing the highest concentrations (69.2 and 119.5 ng g^{-1} (d.w.)) (Table 2). Overall,

PAH concentrations along all cores were relatively constant (Fig. 6). A significant correlation was observed between total PAHs and TOC ($r_s = 0.78$; $p < 0.05$) and grain size ($r_s = 0.81$, $p < 0.05$) in all cores. The individual PAH distribution showed lower concentrations of LMW PAHs and the dominance of HMW PAHs (Table 2), with fluoranthene, pyrene, and benzo[a]anthracene (4 aromatic rings), benzo[b]fluoranthene, benzo[k]fluoranthene, benzo[e]pyrene and indeno[1,2,3-c,d]pyrene (5 rings) and benzo[ghi]perylene (6 rings) being the most abundant PAHs (Fig. 6). All the diagnostic ratios indicated combustion as the main source of PAHs in all 4 cores, in particular combustion of wood, grass, or coal (Fig. 4 and Table 2).

Perylene was the most abundant PAH in all layers of all sediment cores, with concentrations varying from <LOQ to 20.4 ng g^{-1} (d.w.) in cores 1, 2, and 4, and from 26.7 to 62.9 ng g^{-1} (d.w.) in core 3. All samples showed a prevalence of perylene over the $\Sigma 5$ -ring PAHs (more than 69% of perylene), also indicating a predominance of diagenetic sources for the Cassino mud bank (Table 2).

Hydrocarbons distribution

Overall, AHs and PAHs concentrations inside the Patos Lagoon estuary were higher at those sites under the influence of potential sources of hydrocarbons (e.g., sites 2 – 8). These sites are subject to oceanographic conditions (e.g., flocculation), which favor the deposition of hydrocarbons generated in the vicinity of their sources. No significant correlation was observed between the hydrocarbons found in the sites inside the Lagoon and either grain size or TOC, which suggests that source proximity is probably the main cause of hydrocarbon concentration.

Medeiros et al. (2005) have previously assessed hydrocarbon concentrations and sources in 10 out of the 27 sites examined in the present study (sites 1–8, 10 and 26). Compared to the results obtained by Medeiros et al. (2005), the concentrations of PAHs found in the present study were lower at sites 7 and 8 and slightly lower at the other sites, indicating that the study area can still be considered moderate to highly contaminated by hydrocarbons. The contamination levels at these 10 specific sites were similar to those found in other areas considered moderate to highly contaminated with hydrocarbons, such as the

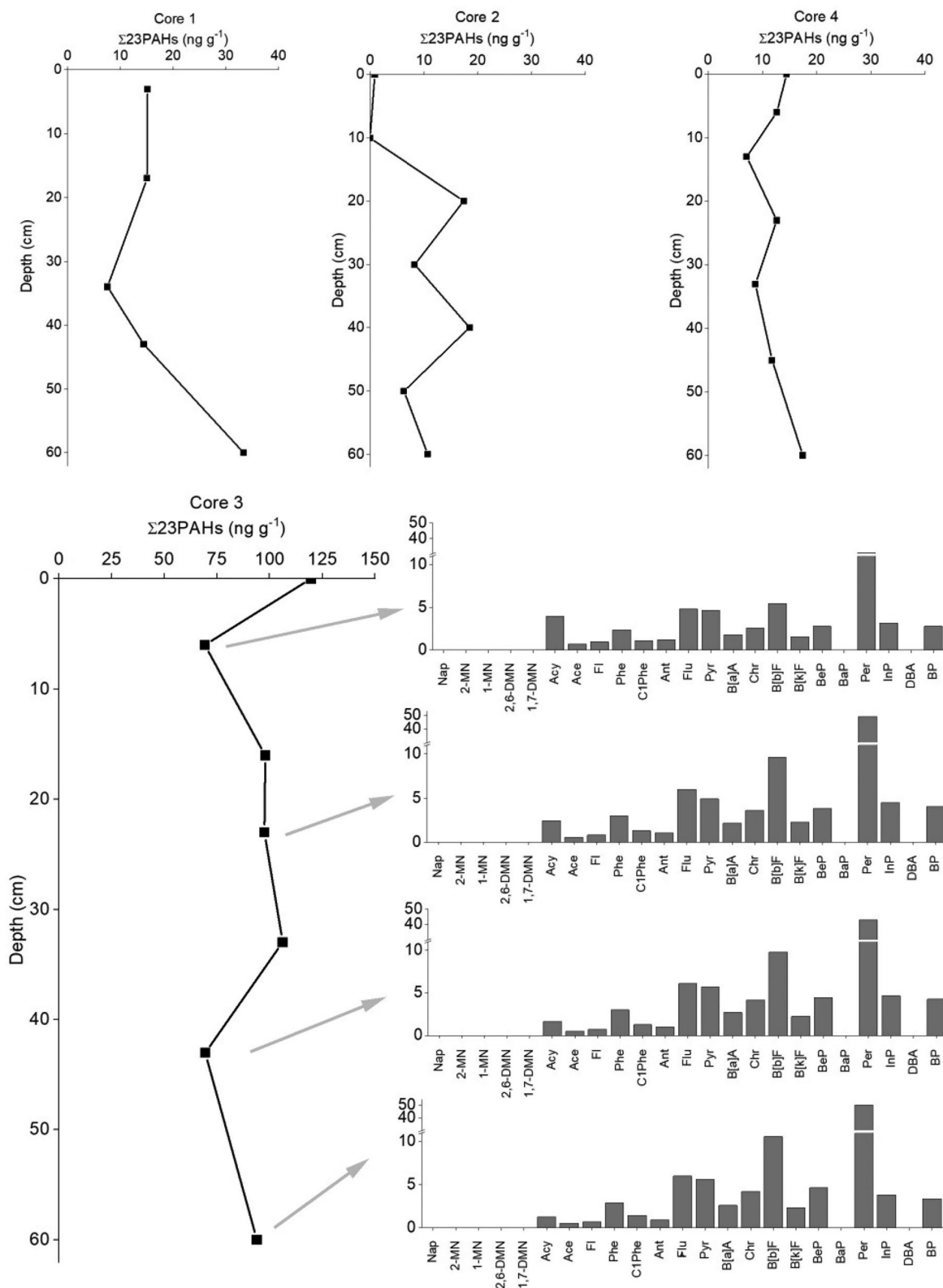


Fig. 6 Sedimentary profile of Σ_{23} PAHs (ng g⁻¹) in the Cassino Beach mud bank sediment cores. The individual distribution of PAHs is presented for the selected profile depth of core 3

Pearl River estuary in China (Zhang et al., 2015), the Iko River estuary mangrove system in Nigeria (Essien et al., 2011) and the Cochin estuary in India (Ramzi et al., 2017).

Intermediate levels of PAHs were observed in sites located along the main navigation channel, directly influenced by maritime activities (sites 18–27). These sites, despite being close to expected sources of PAHs, are subjected to stronger currents (António et al., 2020; Martelo et al., 2019), which apparently can dilute the contamination and/or prevent sediment and hydrocarbon deposition (Janeiro et al., 2008), resulting in the intermediate concentrations observed. Lower AHs and PAHs concentrations were observed in sites located in areas far from the expected sources (sites 1, 11–13) or with low contents of fine sediments, such as Mangueira cove (sites 14–17). Hydrocarbon concentrations at these specific sites were comparable to those found in areas considered uncontaminated, such as Admiralty Bay in Antarctica (Martins et al., 2010) and Laranjeiras Bay (marine protected area) in Brazil (Martins et al., 2012).

Overall, AHs and PAHs concentrations in the Cassino beach mud bank sediment cores were low, much lower than concentrations found near the main hydrocarbon sources at Patos Lagoon estuary (sites 2–10) and similar to concentrations found in sites located in areas far from the expected sources (sites 1, 11–13) or with low content of fine sediments, such as Mangueira cove (sites 14–17). The exception was PAHs in core 3, where concentrations were similar to those seen in sites located in the main navigation channel (19–27). The higher contents of fine sediments and TOC may explain the higher levels of PAHs in core 3. However, the lack of LMW PAHs could also suggest that physical processes of mixing sediment, caused by mud fluidity, promote remobilization or degradation of LMW PAHs, which are more susceptible to this process than HMW PAHs. This may explain why there are low concentrations of LMW PAHs and short-chain *n*-alkanes.

Hydrocarbons inside the Lagoon and in the mud bank seem to have similar sources, showing both biogenic and anthropogenic signatures. Aliphatic hydrocarbons indicated the predominance of terrigenous *n*-alkanes derived

from higher plant waxes and chronic inputs of petrogenic sources. Regarding PAHs composition and diagnostic ratios, pyrogenic PAHs were evidenced inside the Patos Lagoon estuary as well as in the adjacent coastal area.

The Patos Lagoon estuary discharge transports high amounts of suspended material to the adjacent coast, being the main source of sediments to the Cassino beach mud bank (Calliari et al., 2009). Thus, considering the similarity between the levels and profiles of individual hydrocarbons in sediments from the estuary and mud bank, the Patos Lagoon is also the main source of hydrocarbons to the adjacent coastal area. However, all sediment cores showed PAH concentrations below PEL and TEL (Buchman, 2008) and threshold limits set by the Brazilian sediment quality guidelines (Brazil, 2012).

Conclusions

The hydrocarbon individual distribution, as well as the diagnostic ratios, reveals a mixture of natural and anthropogenic inputs inside the Patos Lagoon estuary and in the Cassino Beach mud bank (outside the estuary). Source proximity seems to be the main cause of the hydrocarbon concentrations observed around the study area, with higher hydrocarbon concentrations observed closer to the main potential sources. According to Brazilian and international sediment quality guidelines, 5 sites inside the Lagoon were shown to be moderate to highly contaminated. Nevertheless, the mud transported by storm surges to Cassino Beach shoreface poses minimal risk to local biota and humans, since sediment cores collected in the mud bank showed hydrocarbon concentrations below the threshold limits of sediment quality guidelines. Although depositional history is not registered in the cores due to physical mixing, it is possible to observe that biogenic *n*-alkanes derived from terrestrial plants, *n*-alkanes derived from chronic petrogenic inputs, and pyrolytic PAHs contributions are the predominant sources of hydrocarbons to the samples both inside the estuary and in the mud bank. Since the Patos Lagoon estuary is the main source of suspended sediments to the mud bank and the hydrocarbon signatures were similar in both sampling areas, it can be stated that hydrocarbons (and sediments) originated inside the Lagoon are being transported and deposited on the Cassino beach mud bank.

Acknowledgements The authors thank Dr. Lauro Júlio Calliari (FURG, Brazil, *in memoriam*) for access to the sediment core samples.

Author contribution PAN: conceptualization, sample collection, analysis, writing the first draft; PGC: analysis, review, editing; LCP: sample collection, analysis, review, editing; MRG: sample collection, review, editing; GF: conceptualization, funding, review, editing.

Funding Patricia Neves (MSc grant 133350/2007–0) and Gilberto Fillmann (PQ 312341/2013–0 and 314202/2018–8) were sponsored by CNPq (Brazilian National Research Council). The authors are also grateful to Petrobras for the financial support (Contract No 650.2.386.03.5).

Availability of data and materials All data and materials support the published claims and comply with field standards.

Declarations

Consent for publication All the authors consented to publish this manuscript.

Conflict of interest The authors declare no competing interests.

References

- Ankit, Y., Mishra, P. K., Kumar, P., Jha, D. K., Kumar, V. V., Ambili, V., & Anoop, A. (2017). Molecular distribution and carbon isotope of n-alkanes from Ashtamudi Estuary, South India: Assessment of organic matter sources and paleoclimatic implications. *Marine Chemistry*, 196, 62–70. <https://doi.org/10.1016/j.marchem.2017.08.002>
- Antônio, M. H. P., Fernandes, E. H., & Muelbert, J. H. (2020). Impact of jetty configuration changes on the hydrodynamics of the subtropical Patos Lagoon estuary. *Brazil. Water*, 12, 13197. <https://doi.org/10.3390/w12113197>
- Assunção, M. A., Frena, M., Santos, A. P. S., & dos Santos Madureira, L. A. (2017). Aliphatic and polycyclic aromatic hydrocarbons in surface sediments collected from mangroves with different levels of urbanization in southern Brazil. *Marine Pollution Bulletin*, 119, 439–445. <https://doi.org/10.1016/j.marpolbul.2017.03.071>
- Bakhtiari, A. R., Zakaria, M. P., Yaziz, M. I., Lajis, M. N. H., & Bi, X. (2011). Variations and origins of aliphatic hydrocarbons in sediment cores from Chini Lake in Peninsular Malaysia. *Environmental Forensics*, 12, 79–91. <https://doi.org/10.1080/15275922.2011.547439>
- Bi, X., Sheng, G., Liu, X., Li, C., & Fu, J. (2005). Molecular and carbon and hydrogen isotopic composition of n-alkanes in leaf waxes. *Organic Geochemistry*, 36, 1405–1417. <https://doi.org/10.1016/j.orggeochem.2005.06.001>
- Boldrini, I. I., & Eggers, L. (1996). Grassland vegetation in Southern Brazil: Dynamics of species in cattle excluded areas. *Acta Botanica Brasilica*, 10, 37–50. <https://doi.org/10.1590/S0102-33061996000100004>
- Brasil. (2012). Resolução CONAMA Nº 454, de 01 de novembro de 2012. Estabelece as diretrizes gerais e os procedimentos referenciais para o gerenciamento do material a ser dragado em águas sob jurisdição nacional. Brasília, DF: Conselho Nacional de Meio Ambiente (CONAMA). https://www.icm-bio.gov.br/cepsul/images/stories/legislacao/Resolucao/2012/res_conama_454_2012_materiaisdragadoemaguasjurisdicionaisbrasil.pdf. Accessed on 13 February 2023.
- Buchman, M. F. (2008). *NOAA Screening quick reference tables*. National Ocean and Atmospheric Administration, Office of Response and Restoration Division (NOAA OR & R Report) 08–1. Seattle, USA. <https://repository.library.noaa.gov/view/noaa/9327>. Accessed on 13 February 2023.
- Bueno, C., Figueira, R. C. L., Ivanoff, M. D., Toldo, E. E., Ferreira, P. A. L., Fornaro, L., & Garcia-Rodriguez, R. (2021). Inferring centennial terrigenous input for Patos Lagoon, Brazil: The world's largest choked coastal lagoon. *Journal of Paleolimnology*, 66, 157–169. <https://doi.org/10.1007/s10933-021-00197-7>
- Burchard, H., Schuttelaars, H. M., & Ralston, D. K. (2018). Sediment trapping in estuaries. *Annual Review of Marine Science*, 10, 371–395. <https://doi.org/10.1146/annurev-marine-010816-060535>
- Bush, R. T., & McInerney, F. A. (2015). Influence of temperature and C4 abundance on n-alkane chain length distributions across the central USA. *Organic Geochemistry*, 79, 65–73. <https://doi.org/10.1016/j.orggeochem.2014.12.003>
- Cabral, H., Fonseca, V., Sousa, T., & Costa Leal, M. (2019). Synergistic effects of climate change and marine pollution: An overlooked interaction in coastal and estuarine areas. *International Journal of Environmental Research and Public Health*, 16, 2737. <https://doi.org/10.3390/ijerph16152737>
- Calliari, L. J., Speranski, N. S., Torronteguy, M., & Oliveira, M. B. (2001). The mud banks of Cassino Beach, Southern Brazil: Characteristics, processes and effects. *Journal of Coastal Research*, 318–325. <http://www.jstor.org/stable/25736298>
- Calliari, L. J., Winterwerp, J. C., Fernandes, E. H. L., Cuchiara, D., Vinzon, S. B., Sperle, M., & Holland, K. T. (2009). Fine grain sediment transport and deposition in the Patos Lagoon-Cassino beach sedimentary system. *Continental Shelf Research*, 29, 515–529. <https://doi.org/10.1016/j.csr.2008.09.019>
- Cavalcante, R. M., Sousa, F. W., Nascimento, R. F., Silveira, E. R., & Freire, G. S. S. (2009). The impact of urbanization on tropical mangroves (Fortaleza, Brazil): Evidence from PAH distribution in sediments. *Journal of Environmental Management*, 91, 328–335. <https://doi.org/10.1016/j.jenvman.2009.08.020>
- Chen, C. W., & Chen, C. F. (2011). Distribution, origin, and potential toxicological significance of polycyclic aromatic hydrocarbons (PAHs) in sediments of Kaohsiung Harbor. *Taiwan. Marine Pollution Bulletin*, 63, 417–423. <https://doi.org/10.1016/j.marpolbul.2011.04.047>
- Chevalier, N., Savoye, N., Dubois, S., Lama, M. L., David, V., Lecroart, P., & Budzinski, H. (2015). Precise indices based on n-alkane distribution for quantifying sources of sedimentary organic matter in coastal systems. *Organic Geochemistry*, 88, 69–77. <https://doi.org/10.1016/j.orggeochem.2015.07.006>
- Dauner, A. L. L., Hernandez, E. A., MacCormack, W. P., & Martins, C. C. (2015). Molecular characterisation of anthropogenic sources of sedimentary organic matter

- from Potter Cove, King George Island, Antarctica. *Science of the Total Environment*, 502, 408–416. <https://doi.org/10.1016/j.scitotenv.2014.09.043>
- Essien, J. P., Eduok, S. I., & Olajire, A. A. (2011). Distribution and ecotoxicological significance of polycyclic aromatic hydrocarbons in sediments from Iko River estuary mangrove ecosystem. *Environmental Monitoring and Assessment*, 176, 99–107. <https://doi.org/10.1007/s10661-010-1569-2>
- Farias, C. O., Hamacher, C., de LR Wagener, A., & Scofield, A. D. L. (2008). Origin and degradation of hydrocarbons in mangrove sediments (Rio de Janeiro, Brazil) contaminated by an oil spill. *Organic Geochemistry*, 39, 289–307. <https://doi.org/10.1016/j.orggeochem.2007.12.008>
- Figueiredo, S. A., & Calliari, L. J. (2006). Sedimentologia e suas implicações na morfodinâmica das praias adjacentes às desembocaduras na linha de costa do Rio Grande do Sul. *Gravel*, 4, 73–87. http://www.ufrgs.br/gravel/4/Gravel_4_06.pdf. Accessed on 13 February 2023.
- Foda, M., Hunt, J. R., & Chou, H. T. (1993). A nonlinear model for the fluidization of marine mud by waves. *Journal of Geophysical Research-Oceans*, 98, 7039–7047. <https://doi.org/10.1029/92JC02797>
- Garcia, C. A. E., Evangelista, H., & Möller, O. O. Jr. (2021). Comments on “Dredging in an estuary causes contamination by fluid mud on a tourist ocean beach. Evidence via REE ratios” by N. Mirlean, L. Calliari, and K. Johannesson. In *Marine Pollution Bulletin*, 159(2020), 111495. <https://doi.org/10.1016/j.marpolbul.2020.111495>. *Marine Pollution Bulletin* 166, 112115. <https://doi.org/10.1016/j.marpolbul.2021.112115>
- Garcia, M. R., Mirlean, N., Baisch, P. R., & Caramão, E. B. (2010). Assessment of polycyclic aromatic hydrocarbon influx and sediment contamination in an urbanized estuary. *Environmental Monitoring and Assessment*, 168, 269–276. <https://doi.org/10.1007/s10661-009-1110-7>
- Goswami, P., Ohura, T., Guruge, K. S., Yoshioka, M., Yamanaka, N., Akiba, M., & Munuswamy, N. (2016). Spatio-temporal distribution, source, and genotoxic potential of polycyclic aromatic hydrocarbons in estuarine and riverine sediments from southern India. *Ecotoxicology and Environmental Safety*, 130, 113–123. <https://doi.org/10.1016/j.ecoenv.2016.04.016>
- Gray, J. S., & Elliott, M. (2014). Ecology of marine sediments. Oxford University Press. Hagger, J.A., Depledge, M.H., Galloway, T.S. 2005. Toxicity of tributyltin in the marine mollusc *Mytilus edulis*. *Marine pollution bulletin*, 51, 811–816. <https://doi.org/10.1016/j.marpolbul.2005.06.044>
- Holland, K. T., Vinzon, S. B., & Calliari, L. J. (2009). A field study of coastal dynamics on a muddy coast offshore of Cassino beach. *Brazil Continental Shelf Research*, 29, 503–514 <https://doi.org/10.1016/j.csr.2008.09.023>
- Janeiro, J., Fernandes, E., Martins, F., & Fernandes, R. (2008). Wind and freshwater influence over hydrocarbon dispersal on Patos Lagoon, Brazil. *Marine Pollution Bulletin*, 56, 650–665. <https://doi.org/10.1016/j.marpolbul.2008.01.011>
- Keshavarzifard, M., Zakaria, M. P., Sharifinia, M., Grathwohl, P., Keshavarzifard, S., Sharifi, R., Abbasi, S., & Mehr, M. R. (2020). Determination of hydrocarbon sources in major rivers and estuaries of peninsular Malaysia using aliphatic hydrocarbons and hopanes as biomarkers. *Environmental Forensics*, 23, 255–268. <https://doi.org/10.1080/15275922.2020.1806147>
- Kumar, K. S. S., Nair, S. M., Salas, P. M., Peter, K. J. P., & Kumar, C. S. R. (2016). Aliphatic and polycyclic aromatic hydrocarbon contamination in surface sediment of the Chitrapuzha River, Southwest India. *Chemistry and Ecology*, 32, 117–135. <https://doi.org/10.1080/02757540.2015.1125890>
- Lu, M., Jones, S., McKinney, M., Wagner, R., Ahmad, S. M., Kandow, A., Donahoe, R., Lu, Y.H., 2022. Sources and composition of natural and anthropogenic hydrocarbons in sediments from an impacted estuary. *Science of The Total Environment*, 838, 155779. <https://doi.org/10.1016/j.scitotenv.2022.155779>
- Marangoni, J. C., Costa, C. S. B. (2009). Natural and anthropogenic effects on salt marsh over five decades in the Patos Lagoon (Southern Brazil). *Brazilian Journal of Oceanography*, 57, 345–350. <https://www.scielo.br/j/bjoc/a/rbzWRb4fPHpYYYtVHWZcZRQ/?format=pdf&lang=en>. Accessed on 13 February 2023.
- Martelo, A. F., Trombeta, T. B., Lopes, B. V., Marques, W. C., & Möller, O. O. (2019). Impacts of dredging on the hydromorphodynamics of the Patos Lagoon estuary, southern Brazil. *Ocean Engineering*, 188, 106325. <https://doi.org/10.1016/j.oceaneng.2019.106325>
- Martins, C. C., Bicego, M. C., Figueira, R. C. L., Angelli, J. L. F., Combi, T., Gallice, W. C., Mansur, A. V., Nardes, E., Rocha, M. L., Wisniewski, E., Ceschim, L. M. M., & Ribeiro, A. P. (2012). Multi-molecular markers and metals as tracers of organic matter inputs and contamination status from an Environmental Protection Area in the SW Atlantic (Laranjeiras Bay, Brazil). *Science of the Total Environment*, 417–418, 158–168. <https://doi.org/10.1016/j.scitotenv.2011.11.086>
- Martins, C. C., Doumer, M. E., Gallice, W. C., Dauner, A. L. L., Cabral, A. C., Cardoso, F. D., Dolci, N. N., Camargo, L. M., Ferreira, P. A. L., Figueira, R. C. L., & Mangrich, A. S. (2015). Coupling spectroscopic and chromatographic techniques for evaluation of the depositional history of hydrocarbons in a subtropical estuary. *Environmental Pollution*, 205, 403–414. <https://doi.org/10.1016/j.envpol.2015.07.016>
- Martins, C. C., Seyffert, B. H., Braun, J. F., & Fillmann, G. (2011). Input of organic matter in a large South American tropical estuary (Paranaguá Estuarine System, Brazil) indicated by sedimentary sterols and multivariate statistical approach. *Journal of the Brazilian Chemical Society*, 22, 1585–1594. <https://doi.org/10.1590/S0103-50532011000800023>
- Martins, C. C., Bicego, M. C., Rose, N. L., Taniguchi, S., Lourenço, R. A., Figueira, R. C. L., Mahiques, M. M., & Montone, R. C. (2010). Historical record of polycyclic aromatic hydrocarbons (PAHs) and spheroidal carbonaceous particles (SCPs) in marine sediment cores from Admiralty Bay, King George Island, Antarctica. *Environmental Pollution*, 158, 158–200. <https://doi.org/10.1016/j.envpol.2009.07.025>
- Massone, C. G., de Wagener, A., & L.R., de Abreu, H.M., and Veiga, Á. (2013). Revisiting hydrocarbons source appraisal in sediments exposed to multiple inputs. *Marine Pollution Bulletin*, 73, 345–354. <https://doi.org/10.1016/j.marpolbul.2013.05.043>
- Medeiros, P. M., Bicego, M. C., Castelao, R. M., Rosso, C. D., Fillmann, G., & Zamboni, A. J. (2005). Natural and

- anthropogenic hydrocarbons inputs to sediments of Patos Lagoon Estuary, Brazil. *Environment International*, 31, 77–87. <https://doi.org/10.1016/j.envint.2004.07.001>
- Medeiros, P. M., & Bicego, M. C. (2004). Investigation of natural and anthropogenic hydrocarbon inputs in sediments using geochemical markers. I. Santos, SP—Brazil. *Marine Pollution Bulletin*, 49, 761–769. <https://doi.org/10.1016/j.marpolbul.2004.06.001>
- Meyers, P. A. (1997). Organic geochemical proxies of paleoceanographic, paleolimnologic, and paleoclimatic processes. *Organic Geochemistry*, 27, 213–250. [https://doi.org/10.1016/S0146-6380\(97\)00049-1](https://doi.org/10.1016/S0146-6380(97)00049-1)
- Naidu, R., Biswas, B., Willett, I.R., Cribb, J., Singh, B.K., Nathanail, C.P., Coulon, F., Semple, K. T., Jones, K. C., Barclay, A., & Aitken, R. J. (2021). Chemical pollution: A growing peril and potential catastrophic risk to humanity. *Environment International*, 156, 106616. <https://doi.org/10.1016/j.envint.2021.106616>
- Niencheski, L. F. H., & Fillmann, G. (2006). Contaminantes: Metais, Hidrocarbonetos e Organoclorados. In P. C. Lana, A. Bianchini, C. A. O. Ribeiro, L. F. H. Niencheski, G. Fillmann, C. S. G. Santos (Eds), *Avaliação Ambiental de estuários brasileiros: Diretrizes metodológicas Museu Nacional*, 63–118. ISBN: 8574270172.
- Notar, M., Leskovsek, H., & Faganeli, J. (2001). Composition, distribution and sources of polycyclic aromatic hydrocarbons in sediments of the Gulf of Trieste, Northern Adriatic Sea. *Marine Pollution Bulletin*, 42, 36–44. [https://doi.org/10.1016/S0025-326X\(00\)00092-8](https://doi.org/10.1016/S0025-326X(00)00092-8)
- Oyo-Ita, O. E., Offem, J. O., Ekpo, B. O., & Adie, P. A. (2013). Anthropogenic PAHs in mangrove sediments of the Calabar River, SE Niger Delta, Nigeria. *Applied Geochemistry*, 28, 212–219. <https://doi.org/10.1016/J.APGEOCHEM.2012.09.011>
- Paixao, J. F., de Oliveira, O. M., Dominguez, J. M., Coelho, A. C., Garcia, K. S., Carvalho, G. C., & Magalhaes, W. F. (2010). Relationship of metal content and bioavailability with benthic macrofauna in Camamu Bay (Bahia, Brazil). *Marine Pollution Bulletin*, 60, 474–481. <https://doi.org/10.1016/j.marpolbul.2009.12.002>
- Ramzi, A., Habeeb Rahman, K., Gireeshkumar, T. R., Balachandran, K. K., Jacob, C., & Chandramohanakumar, N. (2017). Dynamics of polycyclic aromatic hydrocarbons (PAHs) in surface sediments of Cochin estuary, India. *Marine Pollution Bulletin*, 114, 1081–1087. <https://doi.org/10.1016/j.marpolbul.2016.10.015>
- Readman, J. W., Fillmann, G., Tolosa, I., Bartocci, J., Villeneuve, J. P., Catinni, C., Mee, L. D. (2002). Petroleum and PAH contamination of the Black Sea. *Marine Pollution Bulletin*, 44, 48–62. [https://doi.org/10.1016/S0025-326X\(01\)00189-8](https://doi.org/10.1016/S0025-326X(01)00189-8)
- Reed, A. H., Faas, R. W., Allison, M. A., Calliari, L. J., Holland, K. T., O'Reilly, S. E., Vaughan, W. C., & Alvez, A. (2009). Characterization of a mud deposit offshore of the Patos Lagoon, Southern Brazil. *Continental Shelf Research*, 29, 597–608. <https://doi.org/10.1016/j.csr.2009.02.001>
- Santos, E., Souza, M. R., Junior, A. R., da Silva Soares, L., Frena, M., & Alexandre, M. R. (2023). Polycyclic aromatic hydrocarbons in suspended particulate matter of a region influenced by agricultural activities in northeast Brazil. *Regional Studies in Marine Science*, 57, 102683. <https://doi.org/10.1016/j.rsma.2022.102683>
- Schefuß, E., Schouten, S., Jansen, J. H. F., & Damsté, J. S. (2003). African vegetation controlled by tropical sea surface temperatures in the mid-Pleistocene period. *Nature*, 422(6930), 418–421. <https://doi.org/10.1038/nature01500>
- Seeliger, U. (2001). The Patos Lagoon Estuary, Brazil. In U. Seeliger, B. Kjerfve (Eds.), *Coastal marine ecosystems of Latin America*. Ecological studies (analysis and synthesis), vol 144. Springer, Berlin, Heidelberg. ISBN: 978–3–662–04482–7.
- Silliman, J. E., Meyers, P. A., & Eadie, B. J. (1998). Perylene: An indicator of alteration processes or precursor materials? *Organic Geochemistry*, 29, 1737–1744. [https://doi.org/10.1016/S0146-6380\(98\)00056-4](https://doi.org/10.1016/S0146-6380(98)00056-4)
- Tobiszewski, M., & Namieśnik, J. (2012). PAH diagnostic ratios for the identification of pollution emission sources. *Environmental Pollution*, 162, 110–119. <https://doi.org/10.1016/j.envpol.2011.10.025>
- Vaezzadeh, V., Zakaria, M. P., Shau-Hwai, A. T., Ibrahim, Z. Z., Mustafa, S., Abootelebi-Jahromi, F., Masood, N., Magam, S. M., & Alkhadher, S. A. A. (2015). Forensic investigation of aliphatic hydrocarbons in the sediments from selected mangrove ecosystems in the west coast of Peninsular Malaysia. *Marine Pollution Bulletin*, 100, 311–320. <https://doi.org/10.1016/j.marpolbul.2015.08.034>
- Varnosfaderany, M. N., Bakhtiari, A. R., Gu, Z., & Chu, G. (2014). Perylene as an indicator of land-based plant biomarkers in the southwest Caspian Sea. *Marine Pollution Bulletin*, 80, 124–131. <https://doi.org/10.1016/j.marpolbul.2014.01.033>
- Vinzon, S. B., Lauro, J. C., Holland, K. T., & Winterwerp, J. C. (2009). On the dynamics of mud deposits in coastal areas. *Continental Shelf Research*, 29, 501–502. <https://doi.org/10.1016/j.csr.2008.09.021>
- Volkman, J. K., Holdsworth, G. D., Neil, G. P., & Bavor, H. J., Jr. (1992). Identification of natural, anthropogenic and petroleum hydrocarbons in aquatic sediments. *Science of the Total Environment*, 112, 203–219. [https://doi.org/10.1016/0048-9697\(92\)90188-X](https://doi.org/10.1016/0048-9697(92)90188-X)
- Wallner-Kersanach, M., Mirlean, N., Baumgarten, M. G. Z., Costa, L. D. F., & Baisch, P. (2016). Temporal evolution of the contamination in the southern area of the Patos Lagoon estuary, RS, Brazil. *Journal of Integrated Coastal Zone Management*, 16, 263–279. <https://doi.org/10.5894/rci596>
- White, K. H., Xu, L., Hartmann, P., Quinn, J. G., & Reddy, C. M. (2013). Unresolved Complex Mixture (UCM) in coastal environments is derived from fossil sources. *Environmental Science and Technology*, 47, 726–731. <https://doi.org/10.1021/es3042065>
- Wu, Y., Jin, R., Chen, Q., Du, X., Yang, J., & Liu, M. (2023). Organic contaminants of emerging concern in global estuaries: Environmental occurrence, fate, and bioavailability. *Critical Reviews in Environmental Science and Technology*, 53, 550–575. <https://doi.org/10.1080/10643389.2022.2077062>
- Yang, J.-P., Liu, X.-P., & Zhang, J.-W. (1998). Distribution of dibenzothiophene in the sediments of the South China Sea. *Environmental Pollution*, 101, 405–414. [https://doi.org/10.1016/S0269-7491\(98\)00020-7](https://doi.org/10.1016/S0269-7491(98)00020-7)
- Yunker, M. B., Macdonald, R. W., Vingarzan, R., Mitchell, R. H., Goyette, D., & Sylvestre, S. (2002). PAHs in the Fraser

- River basin: A critical appraisal of PAH ratios as indicators of PAH source and composition. *Organic Geochemistry*, 33, 489–515. [https://doi.org/10.1016/S0146-6380\(02\)00002-5](https://doi.org/10.1016/S0146-6380(02)00002-5)
- Zhang, J. D., Wang, Y. S., Cheng, H., Jiang, Z. Y., Sun, C. C., & Wu, M. L. (2015). Distribution and sources of the polycyclic aromatic hydrocarbons in the sediments of the Pearl River estuary, China. *Ecotoxicology*, 24, 1643–1649. <https://doi.org/10.1007/s10646-015-1503-z>
- Zou, T., Zhang, H., Meng, Q., & Li, J. (2016). Seasonal hydrodynamics and salt exchange of a shallow estuary in Northern China. *Journal of Coastal Research*, 74, 95–103. <https://doi.org/10.2112/S174-009.1>

Publisher's Note Springer Nature remains neutral with regard to jurisdictional claims in published maps and institutional affiliations.

Springer Nature or its licensor (e.g. a society or other partner) holds exclusive rights to this article under a publishing agreement with the author(s) or other rightsholder(s); author self-archiving of the accepted manuscript version of this article is solely governed by the terms of such publishing agreement and applicable law.